# AN IMPROVED SINGLE PHASE INVERTER POWER CONTROLLER WITH ROOT LOCUS ANALYSYS

**Élcio PRECIOSO DE PAIVA (1); João BATISTA VIEIRA JR. (2); Luís CARLOS DE FREITAS (3); Valdeir JOSÉ FARIAS (4); Ernane ANTÔNIO ALVES COELHO (5).**

(1) Coordenação Área Indústria, Instituto de Federal Educação Tecnológica do Tocantins, AE 310 Sul Av. NS 10 esq, c/ Av. LO-5A, Centro 77021-090 Palmas, TO, Tel. (63) 3225 1205, Fax. (63) 3225 1309, elciopaiva@etfto.gov.br
(2) Laboratório de Eletrônica de Potência, Universidade Federal de Uberlândia
Av. João Naves de Ávila, 1600, Bloco 3N – Câmpus Santa Mônica, 38402 –900 Uberlândia, MG, batista@ufu.br
(3) Laboratório de Eletrônica de Potência, Universidade Federal de Uberlândia
Av. João Naves de Ávila, 1600, Bloco 3N – Câmpus Santa Mônica, 38402 –900 Uberlândia, MG, freitas@ufu.br
(4) Laboratório de Eletrônica de Potência, Universidade Federal de Uberlândia
Av. João Naves de Ávila, 1600, Bloco 3N – Câmpus Santa Mônica, 38402 –900 Uberlândia, MG, farias@ufu.br
(5) Laboratório de Eletrônica de Potência, Universidade Federal de Uberlândia
Av. João Naves de Ávila, 1600, Bloco 3N – Câmpus Santa Mônica, 38402 –900 Uberlândia, MG, ernane@ufu.br

## ABSTRACT

This paper presents an improved controller for a single-phase inverter connected to stiff AC system, which is based on frequency and voltage droops. A new feedback loop is introduced to increase the system damping. The small signal analysis and root locus plots are presented in order to show the connections between the feedback loop gains and behavior of the system. Simulation results corresponding to the numerical solution of the nonlinear system equations are presented to validate the small signal analysis. A description of a laboratory prototype and the respective experimental results are also presented to confirm the theoretical analysis.

Keywords: small signal analysis, inverter paralleling, reactive power control, power control, frequency deviation.

## 1. INTRODUCTION

Dynamic characteristics of a power system can be obtained by small signal analysis using linear techniques, KUNDUR (1994). Stability study of single-phase inverter connected to stiff AC system can be made using the same techniques, (CHANDORKAR et al., 1995) and (COELHO et al., 2000).

The parallel connection control of inverters can be achieved using frequency and voltage droops as can be observed in parallel connection control of synchronous machines, (DIVAN et al., 1991) and (KAWABATA et al., 1998).

Two or more synchronous machines connected in parallel tend to remains in synchronism due to synchronizing torque component. The system stability depends on the existence of sufficient synchronizing and damping torque components. Voltage stability depends on the equilibrium in the demand for reactive power, Kundur.

## 2. CONTROL SCHEME

The control system used to connect the single-phase inverter to stiff AC system is shown in Figure 1. The power calculation block using a computer algorithm obtains both active and reactive powers. In order to increase the system damping a new feedback loop was introduced, that is, an active power deviation from the equilibrium point not only implies a frequency displacement, resulting in an integral action on the phase, but also a direct displacement of the phase of the inverter.

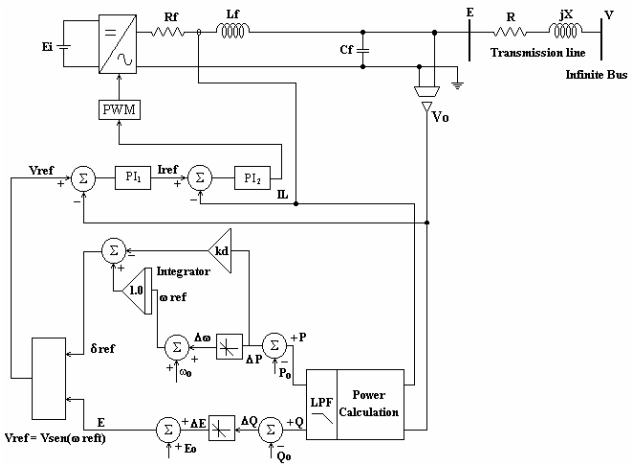


**Figure 1 - Single-phase inverter connected to stiff AC system with the improved controller.**

## 3. SMALL SIGNAL ANALYSIS

Inverter output frequency $\omega$ and inverter output voltage E will be controlled by the droop characteristics defined by (1) e (2), respectively, KUNDUR (1994), which are represented in Figure 2.

$$\omega = \omega_0 - K_p .(P - Po) \quad (1)$$

$$E = E_0 - K_v .(Q - Qo) \quad (2)$$

The active power and the reactive power transfered from the inverter to the stiff AC system are given by (3) and (4), respectively. In this case, these expressions include the power losses and the reactive power through the inductive reactance associated with the transmission line.

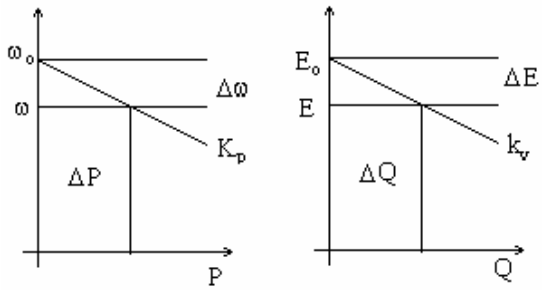


**Figure 2 - Frequency and voltage droops**

Considering small disturbances around the stable equilibrium point defined by ($\delta_e$, $E_e$, $V_e$), the above equations can be linearized, then we have:

$$\Delta\omega = \frac{\partial\omega}{\partial P}\Delta P \quad (5)$$

$$\Delta E = \frac{\partial E}{\partial Q}\Delta Q \quad (6)$$

$$\Delta P = \frac{\partial P}{\partial E}.\Delta E + \frac{\partial P}{\partial \delta}.\Delta\delta \quad (7)$$

$$\Delta Q = \frac{\partial Q}{\partial E}\Delta E + \frac{\partial Q}{\partial \delta}\Delta\delta \quad (8)$$

Where $\Delta$ denotes the small deviation of the variable from the equilibrium point. Substituting for P and Q given by (3) and (4) and calculating the partial derivatives, we obtain:

$$\Delta\delta = -K_D.\Delta P - \frac{K_P.\Delta P}{s} \quad (9)$$

$$\Delta E = -K_V.\Delta Q \quad (10)$$

$$\Delta P = k_{pe}\Delta E + k_{pd}\Delta\delta \quad (11)$$

$$\Delta Q = k_{qe}\Delta E + k_{qd}\Delta\delta \quad (12)$$

where:

$$\text{Kpe} = \frac{1}{\text{R}^2+\text{X}^2}(2RE_e - RV_e\cos\delta_e + XV_e sen\delta_e) \quad (13)$$

$$\text{Kpd} = \frac{1}{\text{R}^2+\text{X}^2}(RE_eV_e sen\delta_e + XE_eV_e\cos\delta_e) \quad (14)$$

$$\text{Kqe} = \frac{1}{\text{R}^2+\text{X}^2}(2XE_e - XV_e\cos\delta_e - RV_e sen\delta_e) \quad (15)$$

$$\text{Kqd} = \frac{1}{\text{R}^2+\text{X}^2}(XE_eV_e sen\delta_e - RE_eV_e\cos\delta_e) \quad (16)$$

The active and reactive output powers obtained by the measuring block can be given by (17) and (18), where $\omega_f$ is the cut-off frequency of the measuring filter.

It is important to take into account that the measuring filter presents a bandwidth much smaller than the inner controllers of the inverter and the system performance will have a hard influence of this fact. In addition, the bandwidth of the inner controllers can be increased using several techniques, (RYAN et al., 1997). Then, we consider the inverter as an ideal voltage source with controllable amplitude and frequency.

$$\Delta\text{P}_{avg}(s) = \frac{\omega_f}{s+\omega_f}\Delta\text{P}(s) \quad (17)$$

$$\Delta Q_{avg}(s) = \frac{\omega_f}{s+\omega_f}\Delta\text{P}(s) \quad (18)$$

Therefore, it follows from above equations:

$$\Delta\delta = -K_D.\frac{\omega_f}{s+\omega_f}.\Delta P - \frac{K_P}{s}.\frac{\omega_f}{(s+\omega_f)}.\Delta P \quad (19)$$

$$\Delta E = -K_V.\left[K_{qe}.\Delta E + K_{qd}.\Delta\delta\right]\frac{\omega_f}{s+\omega_f} \quad (20)$$

$$\Delta E = -\frac{K_V.K_{qd}.\omega_f.\Delta\delta}{s+\omega_f.(1+K_V.K_{qe})} \quad (21)$$

Substituting (9) and (21) in (11) and expanding it, results:

$$\Delta P = \left[ \frac{-K_V . K_{pe} . K_{qd} . \omega_f + K_{pd} . \left( s + \omega_f . \left( 1 + K_V . K_{qe} \right) \right)}{s + \omega_f . \left( 1 + K_V . K_{qe} \right)} \right] . \Delta\delta \qquad (22)$$

Since phase δ is the frequency ω time integral, thus:

$$\Delta\omega(s) = s.\Delta\delta(s) \qquad (23)$$

Substituting (23) in (22) and expanding it, results:

$$s^3\Delta\delta(s) + as^2\Delta\delta(s) + bs\Delta\delta(s) + c\Delta\delta(s) = 0 \qquad (24)$$

Where:

$$a = (\omega_f.(2 + K_V.K_{qe}) + K_D.\omega_f.K_{pd}) \qquad (25)$$

$$b=(\omega_f^2.(1+ K_V.K_{qe}) + K_P.\omega_f.K_{pd} - K_D.K_V.K_{pe}.K_{qd}.\omega_f^2 + K_D.\omega_f^2.K_{pd}.(1 + K_V.K_{qe})) \qquad (26)$$

$$c = K_P.\omega_f^2.(K_{pd}.(1 + K_V.K_{qe}) - K_V.K_{pe}.K_{qd}) \qquad (27)$$

Then, the system response can be analyzed by characteristic equation (28).

$$\lambda^3 + a\lambda^2 + b\lambda + c = 0 \qquad (28)$$

## 4. SIMULATION RESULTS

Some simulations were made in order to validate the small signal model. Two examples for different gain $K_D$ are presented, which emphasize the influence of the feedback from $\Delta P$ to $\Delta\delta$.

### 4.1 Example I

Taking the system showed in Figure 1 with the parameters presented in Table 1, tunning offset of frequency droop and tuning the offset of voltage droop in way that inverter provides the apparent power specified in Table 1, we can obtain the behavior of angle $\Delta\delta$ of the system. Using $K_D = 0$, we have the conventional control showed in (CHANDORKAR et al., 1995), that is, there is no additional damping.

**Table I - System Parameters and Equilibrium Point**

| Variable | Value | Unit |
|---|---|---|
| Line impedance | 0.5+j3.44 | Ω |
| Cut-off freq. of measuring filter (ωf) | 7.54 | rd/s |
| Frequency droop coefficient ωxP (KP) | 0.01 | rd/s/W |
| Voltage droop coefficient ExQ (Kv) | 0.01 | V/VAR |
| **Feedback loop gain of Δδ/ΔP ($K_D$)** | **0** | **rd/W** |
| Apparent power in stiff AC system | 500 + j0 | VA |
| Inverter output apparent power | 510.8+ j74.8 | VA |
| Stiff AC system voltage (V) | 107.2 | V(rms) |
| Inverter output voltage (E) | 110.7 | V(rms) |
| Stiff AC system frequency (ω) | 377 | rd/s |
| Output filter Inductor $L_f$ | 796 | μH |
| Output filter Capacitor $C_f$ | 60 | μF |
| Inverter Switching Frequency $f_S$ | 18 | kHz |

| | | |
|---|---|---|
| DC link Capacitor | 470 | uF |
| Inverter-stiff AC system lead angle ($\Delta\delta$) | 0.1454 | rd |

Solving the characteristic equation (28), we have the following eigenvalues:

$$\lambda_1 = -3.7703 + j15.5986 \quad (29)$$

$$\lambda_2 = -3.7703 - j15.5986 \quad (30)$$

$$\lambda_3 = -9.9677 \quad (31)$$

Considering that initial active and reactive powers are zero, we can obtain the behavior of the system by (24). It is important to keep in mind that (24) provides the deviation from the equilibrium point, and that the behavior of the angle $\delta$ is determined by the following equation:

$$\delta = \delta_{eq.point} + \Delta\delta \quad (32)$$

The system presents two complex conjugated poles and one negative real pole, therefore it presents an oscillatory response. Figure 3 presents the phase response of single-phase inverter connected to stiff AC system obtained from the model described by (24) and simulation in PSpice. The active power and reactive power are presented in figure 4. It can be noticed that reactive power is faster than active power and presents oscillatory response. Figure 5 presents the output voltage and current supplied by inverter.

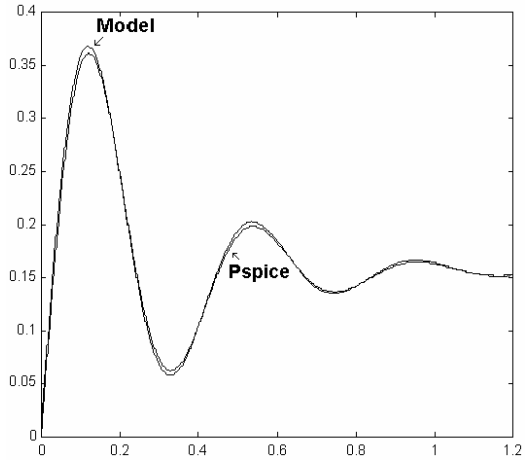


**Figure 3. Phase response of the inverter**

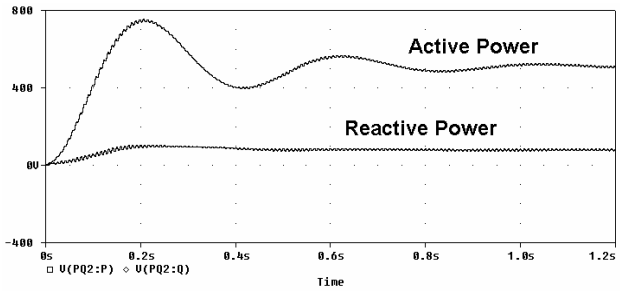


**Figure 4. Active and reactive powers**

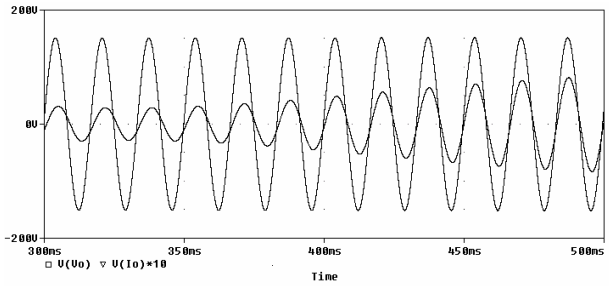


**Figure 5. Output voltage and output current**

## 4.2. Example II

The same parameters from the Example I are used in Example II, except that now $K_D$ = 1e-3, which implies that the new feedback loop is working.

In this case, solving (28), the following eigenvalues are obtained:

$$\lambda_1 = -21.0733 \tag{33}$$

$$\lambda_2 = -12.2200 \tag{34}$$

$$\lambda_3 = -9.9683 \tag{35}$$

It can be noticed that the complex eigenvalues imply that the system presents a damping which is higher than that presented in Example I, as can be observed in Figure 6, where the behavior of the angle $\delta$ obtained by the small signal model and the simulation in PSpice are shown. The results are very close and we can notice that the system is well represented by the small signal model.

The active and reactive powers are shown in Figure 7. Both are oscillatory, but the response is more damped than that obtained in example I.

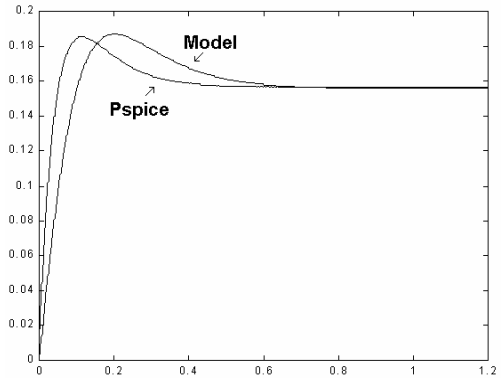


**Figure 6. Phase response of the inverter**

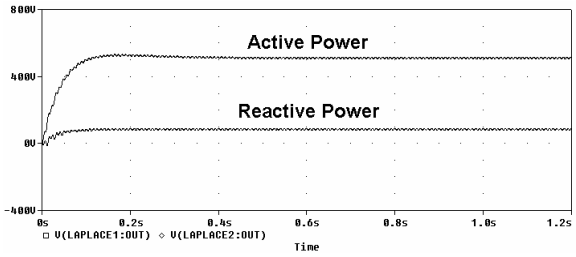


**Figure 7. Active and reactive powers**

Figure 8 presents the output voltage and output current supplied by the inverter.

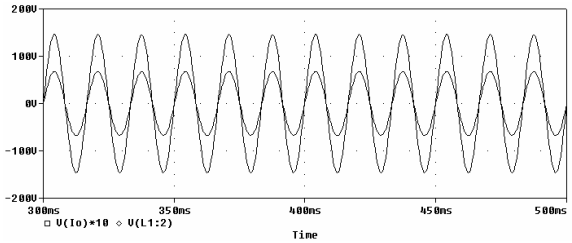


**Figure 8. Output voltage and output current**

## 5. DYNAMIC BEHAVIOR OF THE SYSTEM

In order to understand the dynamic behavior of the system, a root locus plots is shown as a function of the parameter $K_D$.

Figure 9 shows the system root locus plots considering that the droop coefficients $K_p$ and $K_v$ are equal to 0.01 rd/s/W and 0.01 V/VAr, respectively and $K_D$ varies from 0 to 1e-3 rd/W. When $K_D$ = 1e-3, it can be seen that the system presents a damping greater than to $K_D$ = 0, assuming that the proposed model is valid.

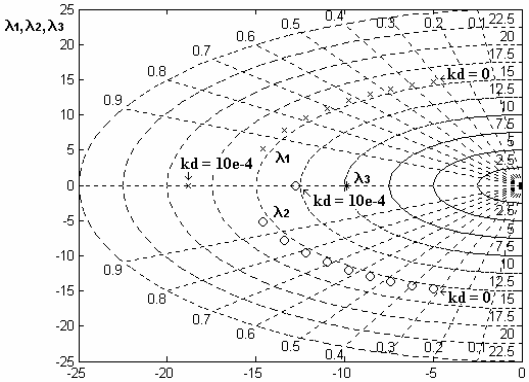


**Figure 9. Root locus plot for $K_p = K_v = 0.01$ and $K_D$ variation from 0 to 0.001**

## 7. EXPERIMENTAL RESULTS

A laboratory prototype was assembled in order to validate the theoretical studies and its parameters are the same of the Table 1. It consists of a single-phase PWM inverter connected to stiff AC system with an inner PI current control loop and an outer PI voltage control loop, as can be seen in Figure 10. First of all, the IGBT gate drivers of the inverter are disabled, and then the switch SW1 is closed. An AC voltage appears in the filter capacitor of the inverter due to the stiff AC system. The reference voltage of the inverter is synchronized with the capacitor voltage by the PLL (*Phase Locked Loop)* block, and then, at 0.1 s after the acquisition system starts saving data, the IGBT gate drivers are enabled and the switch SW2 is changed from state 1 to state 2. Thus, the power flux controller starts working.

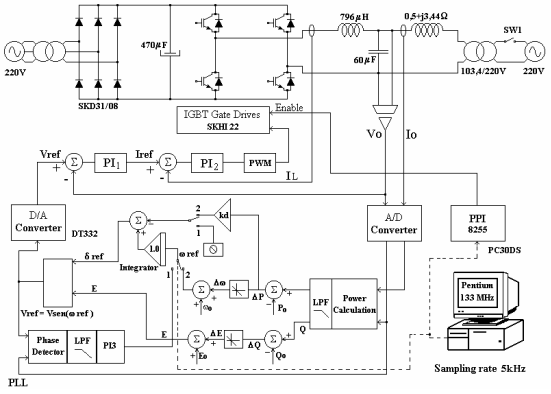


**Figure 10. Laboratory Prototype Scheme**

### 7.1 Analysis for $k_d = 0$

The experimental results with $K_D = 0$ are showed in the figures listed below. In Figure 11, it can be noted that before the inverter being connected with the stiff AC system, the output current and the output voltage have significant distortion because of the harmonic pollution present in the utility system at the point of connection. When the inverter is enabled to work in parallel with the network at instant t = 0.1 s, the output voltage and the output current become significantly more sinusoidal.

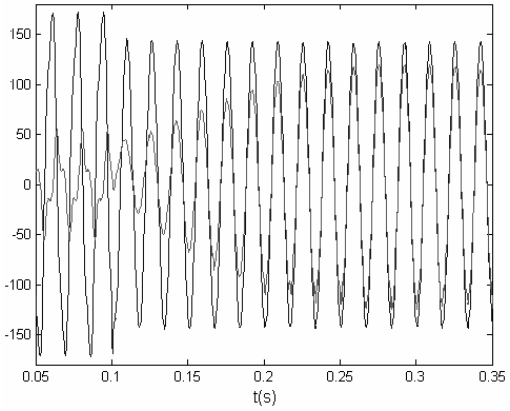


**Figure 11. Output voltage and output current.**

Figure 12 show active and reactive powers that the inverter provides to the ws act stiff AC system with no feedback between $\Delta P$ and $\Delta\delta$, i.e., without the new control loop ($K_D = 0$). In this case, it can be seen that the active power has a quite oscillatory response. The filter capacitor of the inverter provides reactive power for the utility system before the instant that the system is connected to the network, then, the reactive power curve does not start from zero.

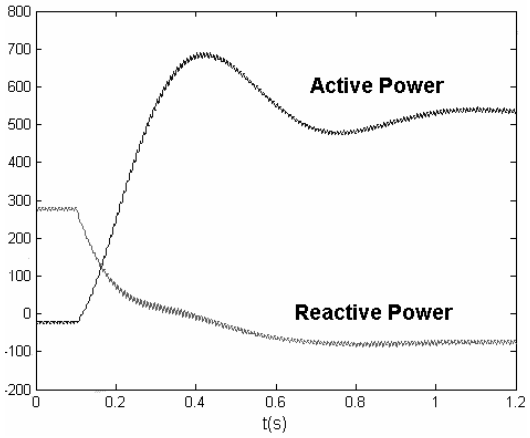


**Figure 12. Active and reactive power ($K_D$=0)**

The following curve represents the inverter frequency during the transient of the connection to the utility system. It can be observed that the frequency has an oscillatory response, as it was expected from the theoretical analysis, since the frequency $\omega$ is the angle $\delta$ derivative in time.

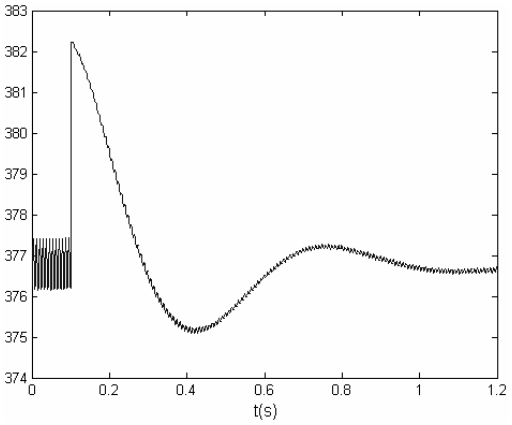


**Figure 13. Inverter frequency ($K_D$=0)**

### 7.2 Analysis for $k_d$ = 0.001

The results achieved using $K_D$ = 1e-3, i.e., with the feedback between $\Delta P$ and $\Delta\delta$ are presented in the following figures.

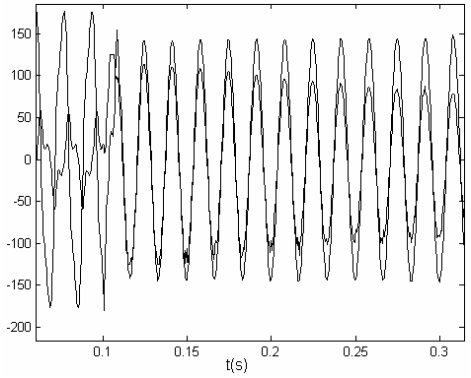


**Figure 14. Output voltage and output current**

**$K_D$ = 1e-3**

It can be seen that the output voltage suffers no overshoot during the transient response.

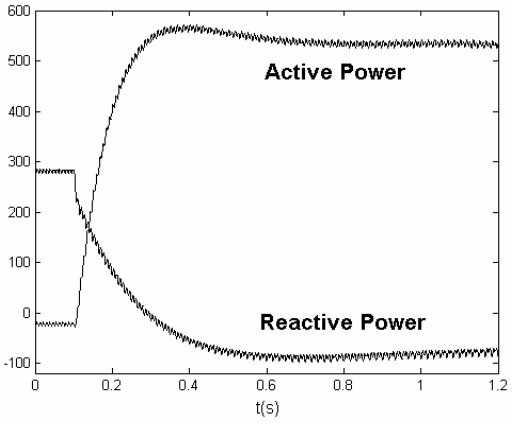


**Figure 15. Active and reactive powers ($K_D$=1e-3)**

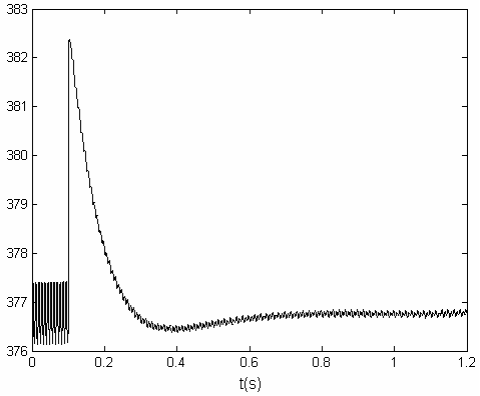


**Figure 16. Inverter frequency ($K_D$=1e-3)**

Figure 16 shows the inverter frequency during the test. The smoothly the frequency changes from its nominal value, the more damped is the oscillation of the active power that is provided to the network. It can also be seen that in both cases, the inverter frequency has a small deviation from the AC stiff system nominal value, $\omega_o$ = 377 rd/s. This is due to the small deviation that occurs in the frequency of the network, since the frequency of the reference voltage is calculated on its basis.

## 8. CONCLUSIONS

This paper has presented a small signal analysis for a single-phase inverter connected to the stiff AC system, which uses an improved power controller. A new feedback loop is proposed to increase the system damping. Simulation results show that the system is well represented by the small signal model.

Several root locus plots as a function of the system parameters can be obtained using the proposed model in order to help designers to define the loop gains for an improved performance of the system.

The control proposed in this paper can be typically applied to cases where inverters are connected to the network in order to convert the power provided by conventional energy sources or even alternative ones.

A prototype of the proposed system was implemented and its experimental results agree with the preceding theoretical analysis. Two cases were analyzed, comparing the controller performance with and without the proposed feedback loop. It was evident the improving in the performance with the new feedback loop working.

## REFERENCES

CHANDORKAR, M.C, **Distributed Uninterruptible Power Supply Systems**. 1995. PhD thesis, University of Wisconsin-Madison, 1995.

COELHO, E. A. A., CORTIZO, P. C., and GARCIA, P. F. D. **Small Signal Stability For Single Phase Inverter Connected to Stiff AC System**, In *IAS 1999*, volume 1. IEEE-IAS, 1999.

COELHO. E.A.A., CORTIZO P.C. and GARCIA, P.F.D. **Small signal stability for parallel connected inverters in stand-alone ac supply systems.** In *IAS2000*, volume CD-ROM, 2000.

DIVAN, D.M., CHANDORKAR, M.C., and ADAPA, R. **Control of parallel connected inverter in stand-alone ac supply systems.** In *IAS'91*. Pages 1003-1009, 1991.

KAWABATA. T. and HIGASHINO. S. **Parallel operation of voltage source inverter,. IEEE Transactions on Industry Applications.** 24(2), Pages 281-287, 1998.

KUNDUR, P. S, *Power System Stability and Control*. McGraw-Hill, Inc., 1994

PAIVA, É. P. **Uma Proposta de Controle de Paralelismo de Inversores com a Rede Elétrica Utilizando-se a Técnica de Realimentação de Fase, Doctorade Thesis.** 2006. 166 p. Thesis – (Doctorade), Federal University of Uberlândia, Uberlândia, 2006.

RYAN, M. J., BRUMSICKLE, W. E., and LORENZ, R. D. **Control topology for single-phase ups inverters, IEEE Transactions On Industry Applications**, 33(2):Pages493-500, 1997.